

# Effect of substrate bias on the microstructure and properties of nanocomposite titanium nitride – based films

M. Dudek <sup>a,b,\*</sup>, O. Zabeida <sup>a</sup>, J.E. Klemburg-Sapieha <sup>a</sup>, L. Martinu <sup>a</sup>

<sup>a</sup> Regroupement québécois sur les matériaux de pointe (RQMP) and Department of Engineering Physics, École Polytechnique de Montréal, Québec, H3C 3A7 Canada

<sup>b</sup> Institute of Materials Science and Engineering, Technical University of Lodz, ul. Stefanowskiego 1/15, 90-924 Łódź, Poland

\* Corresponding author: E-mail address: mardudek@p.lodz.pl

Received 25.09.2009; published in revised form 01.12.2009

## Properties

### ABSTRACT

**Purpose:** Hard nanocomposite nc-TiN/a-SiN films exhibit very attractive mechanical, tribological, optical and electronic properties related to their microstructure and chemical bonding.

**Design/methodology/approach:** In the present work, we investigate ternary thin film TiSiN systems deposited by plasma assisted reactive pulsed magnetron sputtering (PARPMS) from titanium and silicon targets. PARPMS allows one to effectively control ion bombardment by reactive species (e.g.,  $N_2^+$ ,  $N^+$ ) on the surface of the growing film by varying the bias voltage ( $V_B$ ) induced by a radiofrequency (RF) power applied to the substrate.

**Findings:** RF biasing without additional heating of the substrate promotes formation of crystals within the nc films. Specifically, (111) crystal orientation at low  $V_B$  (- 50 V) changed into (200) when  $V_B$  was increased above - 600 V. At the same time, hardness (H) and reduced Young's modulus ( $E_r$ ) of the films changed from  $H \sim 10$  GPa and  $E_r \sim 135$  GPa to their maximum values of  $H \sim 25$  GPa and  $E_r \sim 248$  GPa at  $V_B = - 600$  V. For comparison, for films deposited at 300°C and  $V_B = - 200$  V, the maximum values of H and  $E_r$  of ~ 35 GPa and ~ 350 GPa were observed.

**Practical implications:** The use of the PARPMS to effectively control the mechanical properties and microstructure of transition metal nitride systems films.

**Originality/value:** Discussion of evolution of the film microstructure (crystal size and orientation) at constant film composition and relate it with the energetic aspects of the film growth and film characteristics.

**Keywords:** Mechanical properties; Microstructure; Film growth; Hard nanocomposite films; Transition metal nitride systems; Pulse magnetron sputtering; Ion bombardment

### Reference to this paper should be given in the following way:

M. Dudek, O. Zabeida, J.E. Klemburg-Sapieha, L. Martinu, Effect of substrate bias on the microstructure and properties of nanocomposite titanium nitride – based films, Journal of Achievements in Materials and Manufacturing Engineering 37/2 (2009) 416-421.

## 1. Introduction

Binary and ternary phases, belonging to the transition metal nitride (MeN) systems, have been extensively studied for wear-resistant and protective coating. Recently, much attention has been paid to Si containing films such as TiSiN, CrSiN, and other films systems [1-10]. These films have significantly better mechanical characteristics and oxidation resistance compared to those without Si [11, 12]. The popular out of these films is TiSiN coating, which permit to obtain films with hardness few times higher than typical TiN films. For example Veprek [9] reported the preparation of (Ti, Si)N nanocomposite films by chemical vapour deposition (CVD) method with hardness exceeding 70 GPa. Two main mechanisms have been proposed to explain the hardening observed for adding only a small amount of Si (typically, 1-6 at.%) to MeN system. The first model starting that the nanocomposite systems are formed by small, nanometre size grains embedded in the matrix of polycrystalline or amorphous materials [13, 14]. However the second mechanism attributes hardening to the solid solution effect, where Me atoms are substituted by Si atoms in the MeN lattice [10, 15].

The properties of MeSiN system films are found to be sensitive to growth conditions and hence many different deposition methods have been employed to produce high quality materials; this includes reactive evaporation, ion beam assisted deposition, spray pyrolysis, chemical vapour deposition and magnetron sputtering (MS) [7, 8, 9, 16, 17, 18, 19]. Amongst the different techniques available, the magnetron sputtering method is most widely accepted due to good reproducibility and high film quality.

The most frequently applied parameters to improve properties of sputtered films is increased substrate temperature. The substrate temperature can be replaced by substrate biasing ( $V_B$ ) during the film growth [20, 21]. Both temperature and biasing has led to increase adatom mobility during deposition. Use of mid-frequency pulsing (usually about hundreds of kHz) of DC magnetron discharge (pulse magnetron sputtering, PMS) is another, relatively new way to control the microstructure of films [22]. This method was successfully implemented for the deposition of AlN, TiO<sub>2</sub> and other films [22, 23, 24, 25]. Improvement of film structure and density by pulsing was found for all films, as well as stabilization of the deposition process and significant reduction of arcing at the target were the results in applying a short positive pulsing to the target.

In the present study, we fabricate TiSiN films system using plasma assisted reactive pulsed magnetron sputtering (PARPMS) technique, while creating an additional radio frequency (RF) discharge in the vicinity of the substrate, with the aim to induce ion bombardment of the growing layers, leading to structural changes and the improvement of their characteristics. We evaluated the effect of  $V_B$  at substantially higher values (up to  $V_B = -600$  V) compared to those used by previous authors [7, 8, 26]. The microstructure of the films was determined by X-ray diffraction (XRD). The mechanical properties including nanohardness and Young's modulus were examined.

## 2. Experimental

Silicon doped TiN films were deposited by reactive pulse DC magnetron co-sputtering titanium and silicon (50 mm diameter) targets inclined at 20° with respect to the normal of rotating substrate holder (150 mm diameter). The target-substrate distance was about 100 mm (Fig. 1).

The base pressure in the chamber was lower than 1.3 10<sup>-5</sup> Pa, while total pressure of N<sub>2</sub> and Ar was 1.0 Pa corresponding to a flow of Ar and N<sub>2</sub> of 16 and 0.7 sccm, respectively. The Si content in the films was varied by changing the applied power on Si target ( $P_{Si}$ ) from 50 to 150 W, while maintaining the Ti target power ( $P_{Ti}$ ) at 380 W. The magnetrons were powered from the Pinnacle Plus (Advanced Energy, Inc.) power supply. During the deposition the pulsing frequency ( $f_p$ ) was in the range 50 - 300 kHz with a duty cycle ( $D_c$ ) in the range 50 – 90%. Negative self-bias voltage,  $V_B$ , was controlled by the RF (13.56 MHz) power applied to the substrate holder and changing from 0 to 600 V. The films were deposited on silicon substrate at room temperature and at temperature of 300 °C controlled using a spiral-shaped tubular resistive heater. Optical emission spectra (OES) from magnetron and RF discharge were monitored during deposition using the optical emission spectrometer Ocean Optics.

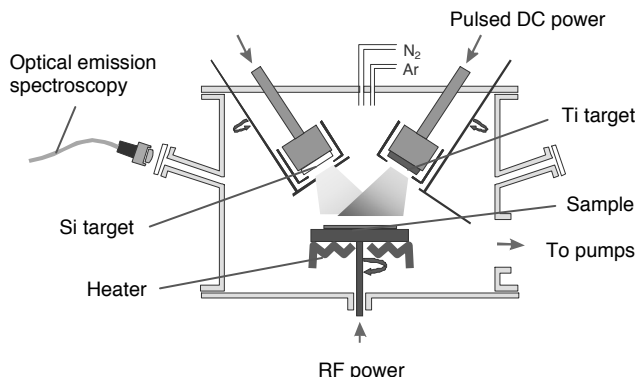


Fig. 1. Schemes of the deposition system

Film microstructure was determined by grazing angle X-ray diffraction (XRD, Philips X'pert diffractometer) at room temperature with an angle of incidence of 0.5°. The XRD patterns were recorded using Cu-K<sub>α</sub> (1.5406 Å) radiation at 50 kV and 40 mA. The diffraction angle was scanned between 20° and 90°, and a divergence slit of 1° was used to obtain strong enough signal for relatively short acquisition times.

Film thickness was measured by step profilometry (Dektak stylus profiler).

The mechanical properties such as hardness ( $H$ ) and Young's modulus ( $E_r$ ) were determined from the load-displacement curves (from 20 indentations) measured by a depth-sensing indentation system (Triboindenter, Hysitron, Inc.), using the approach of Oliver and Pharr [27].

### 3. Results

In the first part of this work, we studied the effect of increasing  $P_{\text{Si}}$  on hardness of TiSiN films. Several deposition processes were performed at various frequencies and duty cycles showed that maximum of  $H$  is obtained at  $P_{\text{Si}} \sim 100$  W. Figure 2 shows the  $H$  and  $E_r$  for films deposited at  $T_s = 300$  °C,  $V_B = -200$  V,  $P_{\text{Ti}} = 380$  W,  $f_p = 300$  kHz,  $D_c = 88\%$  for both Ti and Si target as function of  $P_{\text{Si}}$ . We observe maximum of  $H \sim 35$  GPa and  $E_r \sim 350$  GPa at  $P_{\text{Si}} = 100$  W, which is almost four times lower power supplied to silicon than to titanium target allowed to obtain maximal hardness of deposited films.

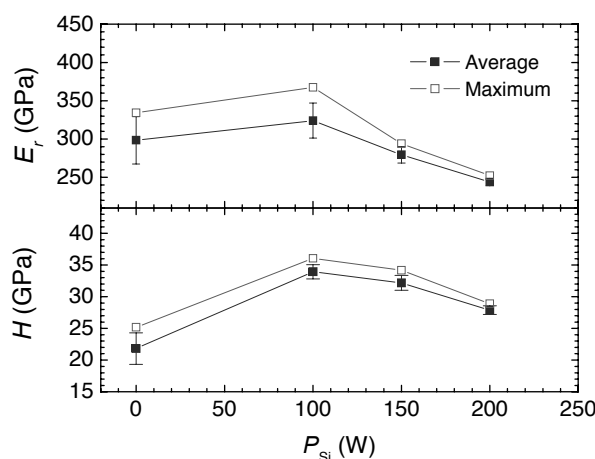


Fig. 2. Effect of  $P_{\text{Si}}$  on  $H$  and  $E_r$  of TiSiN films ( $T_s = 300$  °C,  $V_B = -200$  V,  $P_{\text{Ti}} = 380$  W,  $f_p = 300$  kHz,  $D_c = 88\%$  for both Ti and Si target)

Figure 3 shows XRD patterns of PARPMS TiSiN films deposited under various  $P_{\text{Si}}$  with previously indicated condition. It shows characteristic diffraction pattern of pure TiN, with (111) and (200) principal orientations, and small peaks due to (220), (311) and (222) orientations. All TiN peaks appear on the low angle side of the strain-free reference material (JCPDS powder diffraction database), indicating presence of the compressive stress in the coating. Addition of Si exhibits very similar XRD patterns. The grain size of the films changed from  $D_{111} = 11.7$  nm and  $D_{200} = 10.7$  nm at  $P_{\text{Si}} = 0$  W to values of  $D_{111} = 11.4$  nm and  $D_{200} = 9.3$  nm at  $P_{\text{Si}} = 100$  W. This indicates that the crystals become ‘diluted’ (increased separation) with Si co-sputtering and we observe increase of hardness from  $\sim 22$  to  $\sim 34$  GPa.

Further increase of Si contents leads to reduction of grain size and change crystal orientation of TiSiN films. It is interesting that at  $P_{\text{Si}} > 150$  W intensity of (200) peaks decreased to a very low value close to zero. Simultaneously, at higher Si content broadening the (111) and (200) peaks is observed. It is a sign of increase in the amount of Si atoms substituting Ti atoms in the  $\text{TiN}_{1-x}$  lattice, and thus, increase of the  $\text{Si}_3\text{N}_4$  phase fraction.

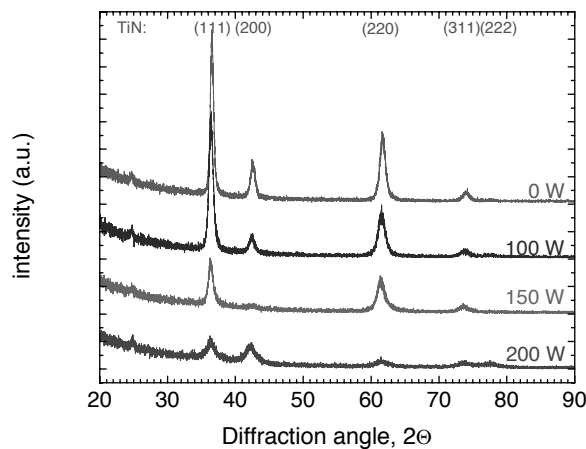


Fig. 3. XRD patterns of TiSiN films deposited at various  $P_{\text{Si}}$  ( $T_s = 300$  °C,  $V_B = -200$  V,  $P_{\text{Ti}} = 380$  W,  $f_p = 300$  kHz,  $D_c = 88\%$  for both Ti and Si target)

Effect of  $f_p$  and  $D_c$  on microstructure and mechanical properties was also investigated. For fixed pulsed parameters applying to Ti target ( $P_{\text{Ti}} = 380$  W,  $f_p = 300$  kHz and  $D_c = 88\%$ ) and optimal  $P_{\text{Si}} = 100$  W,  $H$  and  $E_r$  of TiSiN films were independent on pulsing parameters applied to Si target, and achieve values of  $H \sim 35$  GPa and  $E_r \sim 350$  GPa. When decreasing  $f_p$  applied to Ti target from 300 kHz to 50 kHz ( $D_c = 90\%$ ) the value of  $H$  and  $E_r$  drop to  $\sim 17$  GPa and  $\sim 250$  GPa. We do not observe significant effect on  $H$  and  $E_r$  by changing  $V_B$  (Fig. 4). To understand this effect we repeat this experiment for films deposited at room temperature.

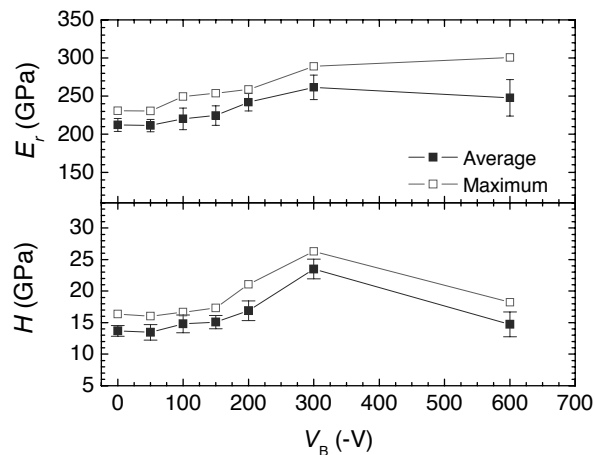


Fig. 4. Effect of  $V_B$  on  $H$  and  $E_r$  ( $P_{\text{Ti}} = 380$  W,  $P_{\text{Si}} = 100$  W,  $T_s = 300$  °C,  $f_p = 50$  kHz,  $D_c = 90\%$  for both Ti and Si target)

The effect of the substrate biasing  $V_B$  on  $H$  and  $E_r$  of films deposited at room temperature ( $P_{\text{Ti}} = 380$  W,  $P_{\text{Si}} = 100$  W,  $f_p = 50$  kHz,  $D_c = 90\%$  for both Ti and Si target) is shown in Fig. 5. Increasing the negative substrate bias from 0 to  $V_B = -600$  V caused a steady increase of  $H$  from 10 GPa to  $\sim 25$  GPa and  $E_r$

from 130 GPa to about 248 GPa. The main reason for low  $H$  value is low deposition temperature [4, 5, 8, 14, 15].

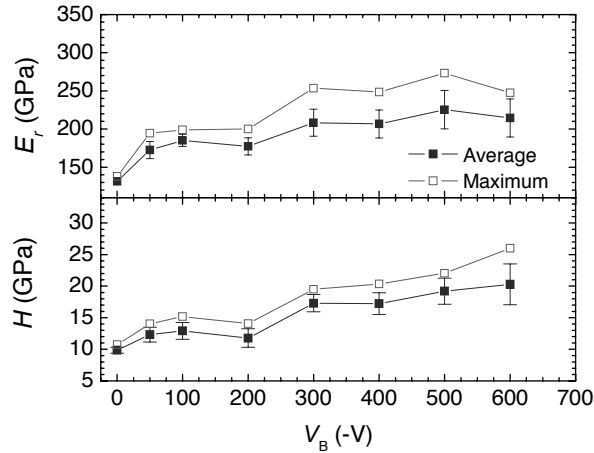


Fig. 5.  $H$  and  $E_r$  vs.  $V_B$  for films deposited at room temperature ( $P_{Ti} = 380$  W,  $P_{Si} = 100$  W,  $f_p = 50$  kHz,  $D_c = 90\%$  for both Ti and Si target)

XRD patterns for the sample deposited at various substrate biases is shown in Fig. 6. As expected, the film deposited without bias is amorphous. Three small peaks observed in spectra can be attributed to silicon substrate. At low substrate bias we observe (111) and (200) peaks. With increasing bias intensity of those peaks changes, and at  $V_B = -300$  V we can observe in addition the change of (111) orientation onto (200), which is symptomatic of densification of TiN-containing films, observed under intense ion bombardment [16, 17].

Thin films deposited at  $V_B = 0$  V at the absence of the ion bombardment and the low deposition temperature do not provide the necessary mobility to stimulate grain growth and renucleation processes necessary to deposit hard nanocomposite films [1], what was confirmed by [7, 8, 18].

By increasing  $V_B$  we observe increase in intensity of (111) and (200) peaks at Fig. 6. This can be related to formation of  $Ti_{1-x}Si_xN_y$  phase, prior described by Vaz et al. [7, 8], where some of the Si atoms occupied Ti position in the fcc TiN lattice. Farther increase of  $V_B$  cause increase of (200) peak intensity at the expense of (111) peak, leading to formation of TiN polycrystalline grains embedded in amorphous silicon nitride tissue.

Estimated the films crystal size using the Debye-Sherrer equation (Fig. 7) shows that these value at (200) crystal orientation steady increase achieving maximum 5.6 nm crystal size at  $V_B = -500$  V, at which the (111) crystal orientation is minimal. This may be due to stopping grain growth as the result of phase segregation between the crystalline and amorphous materials [18]. The  $H$  of the TiSiN film with that crystal size and orientation is the biggest ~ 22 GPa.

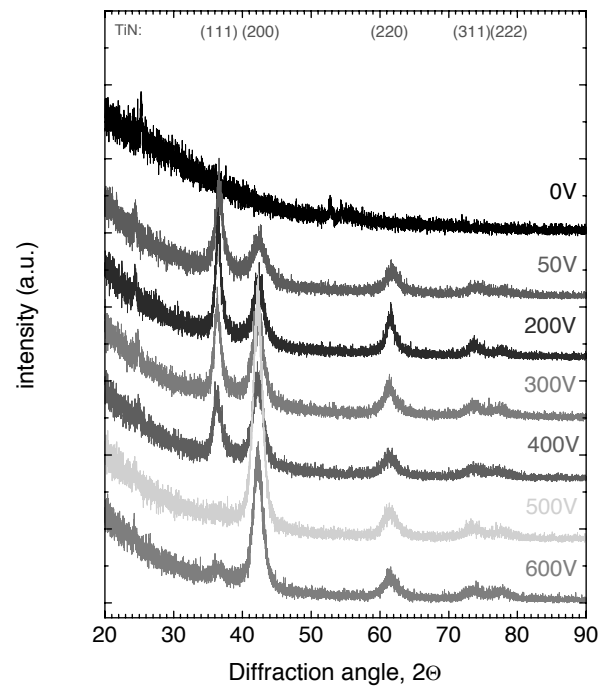


Fig. 6. XRD patterns of TiSiN films deposited at various  $V_B$

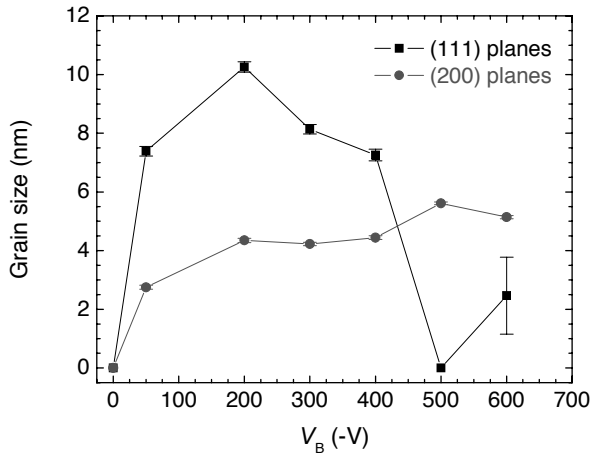


Fig. 7. Effect of  $V_B$  on films crystal size estimated at (111) and (200) orientation

The RF glow discharge in the vicinity of the substrate strongly influence sputtering process and characteristic of the TiN films doped by silicon. Improvement in film mechanical properties is not primarily due to a substrate heating effect, but an increased flux of atomic nitrogen and sputtering atoms to the growing surface.

Analysis of optical emission spectra (not shown here) performed during the film grow process shows that intensity of Ti lines increase steady with  $V_B$ . However, intensity of N line (336.734 nm) initially increases  $V_B$ , achieving maximum at

$V_B = -500$  V, and then slowly decrease. This behaviour is symptomatic changing the crystallographic structure, increase of (200) peak intensity and completed disappear grain size of (111) crystal orientation. The quenching of N species at higher substrate bias is not well understood. It may probably be due to decrease of the mean free path of N atoms. Nevertheless, higher intensity of 336.734 nm nitrogen line observed at high bias can be considered as additional source of reactive atoms leading to more efficient nitrogen incorporation and defect passivation. It is worth mentioning that no optical emission of  $\text{Si}^+$  ions was identified, which was most probably masked by argon or nitrogen emissions.

## 4. Conclusions

This work has demonstrated that the presence of RF glow discharge at the substrate leads to change of crystal orientation and mechanical properties of TiSiN films deposited by reactive pulse magnetron sputtering.

The PARPMS process produces thin films with the maximum values of  $H$  and  $E_r$  of  $\sim 35$  GPa and  $\sim 350$  GPa obtained at  $300^\circ\text{C}$  and  $V_B = -200$  V. This result confirmed that higher frequency applied to the target ( $f_p = 300$  kHz) and duty cycle 90% are an optimal pulse condition for deposition of MeSiN system films [15].

In comparison with other studies, low hardness and strong (111) crystal orientation observed at low  $V_B$  can be attributed to relatively high pressure (1.0 Pa) during growth of titanium nitride-based films [28, 29, 30]. Experiments with lower pressure during deposition should be performed for better understanding of the role of addition of RF glow discharge at the substrate during co-sputtering process at room temperature. Particularly, changing crystal orientation from (111) onto (200) at  $V_B = -300$  V, which indicate densification of TiN films under intense ion bombardment. Finally, it is necessary to emphasize that the effect of RF glow discharge at the substrate is strongly correlated with substrate temperature.

## Acknowledgements

The authors wish to thank Dr Paweł Jedrzejowski and Mr. Etienne Bousser for nanoindentation measurements as well as numerous fruitful discussions. We also acknowledge the expert technical assistance of Mr. Francis Turcot. This project was supported in part by the NSERC of Canada Strategic Grant Program. M.D. acknowledges the NATO/NSERC Fellowship.

## References

- [1] S. Veprek, Conventional and new approaches towards the design of novel superhard materials, *Surface and Coatings Technology* 97 (1997) 15-22.
- [2] L.A. Dobrzański, L. Wosińska, J. Mikuła, K. Gołombek, T. Gawarecki, Investigation of hard gradient PVD (Ti,Al,Si)N coating, *Journal of Achievements in Materials and Manufacturing Engineering* 24/1 (2007) 59-62.
- [3] L.A. Dobrzański, K. Lukaszkowicz, J. Mikuła, D. Pakuła, Structure and corrosion resistance of gradient and multilayer coatings, *Journal of Achievements in Materials and Manufacturing Engineering* 18 (2006) 75-78.
- [4] M. Ahlgren, H. Blomqvist, Influence of bias variation on residual stress and texture in TiAlN PVD coatings, *Surface and Coatings Technology* 200 (2005) 157-160.
- [5] K. Yamamoto, S. Kujime, K. Takahara, Structural and mechanical property of Si incorporated (Ti,Cr,Al)N coatings deposited by arc ion plating process, *Surface and Coatings Technology* 200 (2005) 1383-1390.
- [6] K. Lukaszkowicz, L.A. Dobrzański, M. Pancielejko, Mechanical properties of the PVD gradient coatings deposited onto the hot work tool steel X40CrMoV5-1, *Journal of Achievements in Materials and Manufacturing Engineering* 24/2 (2007) 115-118.
- [7] F. Vaz, L. Rebouta, P. Goudeau, J. Pacaud, H. Garem, J.P. Riviere, A. Cavaleiro, E. Alves, Characterization of  $\text{Ti}_{1-x}\text{Si}_x\text{N}_y$  nanocomposite films, *Surface and Coatings Technology* 133-14 (2000) 307-313.
- [8] F. Vaz, L. Rebouta, Ph. Goudeau, T. Girardeau, J. Pacaud, J.P. Riviere, A. Traverse, Structural transitions in hard Si-based TiN coatings: The effect of bias voltage and temperature, *Surface and Coatings Technology* 146-147 (2001) 274-279.
- [9] S. Veprek, S. Reiprich, Concept for the design of novel superhard coatings, *Thin Solid Films* 268 (1995) 64-71.
- [10] E. Martinez, R. Sanjines, O. Banakh, F. Levy, Electrical, optical and mechanical properties of sputtered  $\text{CrN}_y$  and  $\text{Cr}_{1-x}\text{Si}_x\text{N}_{1.02}$  thin films, *Thin Solid Films* 447-448 (2004) 332-336.
- [11] S. Veprek, M. Veprek-Heijman, P. Karvánková, J. Prochazka, Different approaches to superhard coatings and nanocomposites, *Thin Solid Films* 476 (2005) 1-29.
- [12] M. Polok-Rubiniec, L.A. Dobrzański, K. Lukaszkowicz, M. Adamiak, Comparison of the structure, properties and wear resistance of the TiN PVD coatings, *Journal of Achievements in Materials and Manufacturing Engineering* 27/1 (2008) 87-90.
- [13] S. Veprek, The search for novel, superhard materials, *Journal of Vacuum Science and Technology A* 17 (1999) 2401-2420.
- [14] A. Niederhofer, P. Nesladek, H.-D. Mannling, K. Moto, S. Veprek, M. Jilek, Structural properties, internal stress and thermal stability of nc-TiN/a-Si<sub>3</sub>N<sub>4</sub>, nc-TiN/TiSi<sub>x</sub> and nc-(Ti<sub>1-y</sub>Al<sub>y</sub>Si<sub>x</sub>)N superhard nanocomposite coatings reaching the hardness of diamond, *Surface and Coatings Technology* 120-121 (1999) 173-178.
- [15] M. Benkahoul, P. Robin, S.C. Gujrathi, L. Martinu, J.E. Klemburg-Sapieha, Microstructure and mechanical properties of Cr-Si-N coating prepared by pulsed reactive dual magnetron sputtering, *Surface and Coatings Technology* 202 (2008) 3975-3980.
- [16] L. Shizhi, S. Yulong, P. Hongrui, Ti-Si-N films prepared by plasma-enhanced chemical vapour deposition, *Plasma Chemistry and Plasma Processing* 12 (1992) 287-297.
- [17] J.E. Greene, J.-E. Sundgren, L. Hultman, I. Petrov, D.B. Bergstrom, Development of preferred orientation in polycrystalline TiN layers grown by ultrahigh vacuum

- reactive magnetron sputtering, *Applied Physics Letter* 67 (1995) 2928-2930.
- [18] P. Jedrzejowski, J.E. Klemberg-Sapieha, L. Martinu, Relationship between the mechanical properties and the microstructure of nanocomposite TiN/SiN<sub>1.3</sub> coatings prepared by low temperature plasma enhanced chemical vapour deposition, *Thin Solid Films* 426 (2003) 150-159.
- [19] M. Nose, Y. Deguchi, T. Mae, E. Honbo, T. Nagae, K. Nogi, Influence of sputtering conditions on the structure and properties of Ti-Si-N thin films prepared by r.f.-reactive sputtering, *Surface and Coatings Technology* 174-175 (2003) 261-265.
- [20] A. Amassian, M. Dudek, O. Zabeida, S. Gujrathi, J.E. Klemberg-Sapieha, L. Martinu, Oxygen incorporation and charge donor activation via subplantation during growth of indium tin oxide films, *Journal of Vacuum Science and Technology A* 27 (2009) 362-366.
- [21] M. Dudek, A. Amassian, O. Zabeida, J.E. Klemberg-Sapieha, L. Martinu, Ion bombardment-induced enhancement of the properties of indium tin oxide films prepared by plasma-assisted reactive magnetron sputtering, *Thin Solid Films* 517 (2009) 4576-4582.
- [22] S. Schiller, K. Goedicke, J. Reschke, V. Kirchhoff, S. Schneider, F. Milde, Pulsed magnetron sputter technology, *Surface and Coatings Technology* 61 (1993) 331-337.
- [23] A. Belkind, A. Freilich, R. Scholl, Using pulsed direct current power for reactive sputtering of Al<sub>2</sub>O<sub>3</sub>, *Journal of Vacuum Science and Technology A* 17 (1999) 1934-1940.
- [24] D.A. Glocker, Influence of the plasma on substrate heating during low-frequency reactive sputtering of AlN, *Journal of Vacuum Science and Technology A* 11 (1993) 2989-2993.
- [25] A.I. Rogozin, M.V. Vinnichenko, A. Kolitsch, W. Moller, Effect of deposition parameters on properties of ITO films prepared by reactive middle frequency pulsed dual magnetron sputtering, *Journal of Vacuum Science and Technology A* 22 (2004) 349-355.
- [26] P. Patsalas, C. Charitidis, S. Logothetidis, The effect of substrate temperature and biasing on the mechanical properties and structure of sputtered titanium nitride thin films, *Surface and Coatings Technology* 125 (2000) 335-340.
- [27] W.C. Oliver, G.M. Pharr, Improved technique for determining hardness and elastic modulus using load and displacement sensing indentation experiments, *Journal of Materials Research* 7 (1992) 1564-1583.
- [28] J.E. Carsley, J. Ning, W.W. Milligan, S.A. Hackney, E.C. Aifantis, A simple, mixtures-based model for the grain size dependence of strength in nanophase metals, *Nanostructured Materials* 5 (1995) 441-448.
- [29] Y. Ando, I. Sakamoto, I. Suzuki, S. Maruno, Resistivity and structural defects of reactively sputtered TiN and HfN films, *Thin Solid Films* 343-344 (1999) 246-249.
- [30] T.-Sh. Yeh, J.-M. Wu, L.-J. Hu, The properties of TiN thin films deposited by pulsed direct current magnetron sputtering, *Thin Solid Films* 516 (2008) 7294-7298.